

# PASSBAND MODES EXCITATION TRIGGERED BY FIELD EMISSION IN ESS MEDIUM BETA CAVITY PROTOTYPE

J.F. Chen<sup>†</sup>, M. Bertucci, A. Bosotti, P. Michelato, L. Monaco, R. Paparella, D. Sertore,  
INFN-LASA, Segrate (MI), Italy

S. Pirani<sup>1</sup>, T.P.Å Åkesson, M. Eshraqui, M. Lindroos, ESS, Lund, Sweden

<sup>1</sup>on leave at INFN-LASA, Segrate (MI), Italy

C. Pagani, Università degli Studi di Milano & INFN Milano - LASA, Segrate (MI), Italy

## Abstract

During the first vertical test of ESS Medium-Beta large-grain prototype cavity in INFN-LASA, a phenomenon of coexisting two passband-modes was observed:  $4/6 \pi$  mode was excited spontaneously during the power rise of  $3/6 \pi$  mode. This phenomenon, probably the first time seeing a passband mode excited from non-accelerating mode, is most likely due to the field-emission electrons that transfer their energy gained from the  $3/6 \pi$  mode to the  $4/6 \pi$  mode. In this paper, we present the experimental results, the excitation mechanism and the related simulation results.

## INTRODUCTION

As an in-kind contribution to the ESS project, INFN-LASA is in charge of the development and of the industrial production of the whole set of 36 medium-beta (MB) resonators. Two cavity prototypes, with same geometry but different materials, have been realized: one is in Fine Grain (FG) niobium, i.e. the standard technology for SC cavities and the other in Large Grain (LG) niobium.

Among their vertical tests at LASA, the two cold tests of FG cavity prototype, before and after tank welding, respectively, show excellent performance with low field emission (FE) [1].

Also, the LG cavity was cold tested two times and in both cases, it quenched at about 10 MV/m. In the first test, the quench was accompanied by strong field emission and Multipacting measured via x-ray radiation detectors [2, 3]. Moreover, the simultaneous presence of two passband-modes was observed:  $4/6 \pi$  mode was excited spontaneously during the power rise of  $3/6 \pi$  mode. After the 1<sup>st</sup> test, the cavity was treated with an additional flash BCP and a long 24-hour HPR to cure the strong field emission observed [2]. In the 2<sup>nd</sup> test, the cavity quenched at same field level but with very low field emission, and the phenomenon of passband-mode excitation was not observed anymore.

This passband-mode excitation is most likely due to field-emitted electrons that transfer their energy, gained from the main mode, to the secondary mode. With a similarity to the phenomenon observed in the TESLA cavities in which the  $7/9 \pi$  mode is excited during the power rise of  $\pi$  mode [4], the passband mode excitation in ESS MB cavity is observed, probably the first time in an elliptical cavity triggered by a non-accelerating mode. Therefore, it is of interest to study the electrons' behaviour and the

triggering condition of this passband mode excitation in the ESS MB cavity.

## EXPERIMENTAL OBSERVATION

In order to study the location of field emitters, the cavity has been tested in all the other five-passband modes during its first test at cold. During the power rise of  $3/6 \pi$  mode, another mode with higher frequency but lower transmitted power, -28 dB, was observed on the screen of the spectrum analyzer, as shown in Figure 1. According to the frequencies distribution of the 1<sup>st</sup> monopole band in ESS MB cavity [5], this mode is confirmed as  $4/6 \pi$  mode.

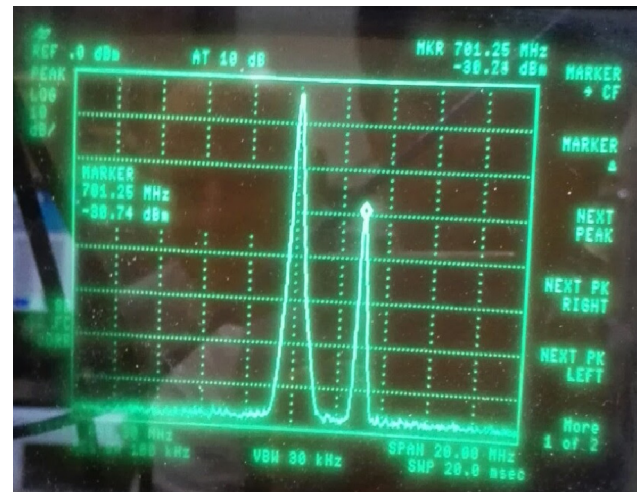


Figure 1: Passband excitation was observed in the 1<sup>st</sup> test at cold of our ESS MB prototype LG cavity (high peak:  $3/6 \pi$  mode; low peak:  $4/6 \pi$  mode).

This phenomenon occurred close to the quench field level in  $3/6 \pi$  mode, accompanied by strong FE. Figure 2 shows the  $Q_0$  vs  $E_{acc}$  result of LG cavity in  $3/6 \pi$  mode, where the reported accelerating field value is scaled to represent the maximum accelerating field in this mode. According to the test result, the maximum equivalent accelerating field is about 10 MV/m, corresponding to a maximum on-axis field about 20 MV/m. The field relationship of the modes can be calculated by

$$E_2/E_1 = \sqrt{P_2/P_1} \approx 0.04$$

where  $P_1$  and  $P_2$  are transmitted power of  $3/6 \pi$  mode and  $4/6 \pi$  mode, respectively, measured by the spectrum in dBm. Given the field of triggering mode and the difference of two transmitted powers, the maximum on axis field of excited mode can be estimated at about 1 MV/m.

<sup>†</sup>jinfang.chen@mi.infn.it

Content from this work may be used under the terms of the CC BY 3.0 licence (© 2017). Any distribution of this work must maintain attribution to the author(s), title of the work, publisher, and DOI.

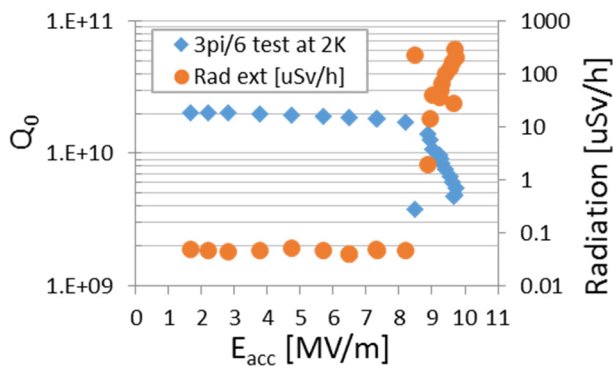


Figure 2: LG cavity tested in  $3/6 \pi$  mode during 1<sup>st</sup> cooling down.

### SIMULATION

Generally, FE occurs in highest surface electric field ( $E_s$ ) regions that are located near irises. Since the cavity is symmetric to the central iris of the cavity, only 4 irises (marked as iris 0 to iris 3) of the left half cavity are taken for the simulation. Hence, all the simulation results adopt to the other half cavity just with a mirror symmetry.

Differently from  $\pi$ -mode, the maximum  $E_s$  of  $3/6 \pi$  mode are not always in the iris centre. Figure 3 shows the  $E_s$  along the cavity axis together with the cavity profile, in which the centres of iris-1 and iris-3 show a quasi-zero  $E_s$ . This  $E_s$  profile is used as a criterion to choose the possible emission sites in the following work.

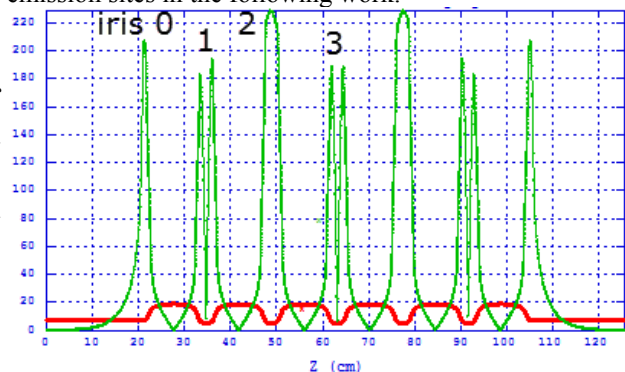


Figure 3: Surface electric fields of  $3/6 \pi$  mode in ESS MB cavity.

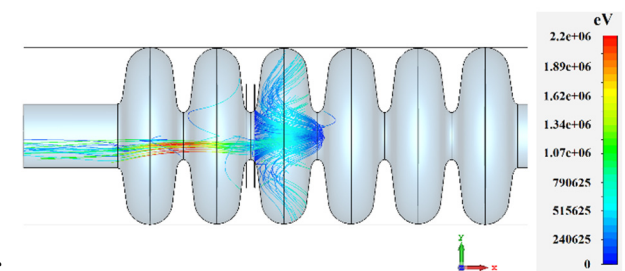


Figure 4: Acceleration and deceleration of electrons emitted from 2<sup>nd</sup> inner iris, in the field of only  $3/6 \pi$  mode of ESS-MB cavity.

As mentioned above, the passband mode excitation is most likely due to the field-emission electrons that are accelerated to high energy by the driving mode, and then

decelerated to lower energy, transferring their energy to the excited mode [6, 7]. We simulated the electrons trajectories only for the  $3/6 \pi$  mode field by CST [8] in full 3D. As shown in Figure 4, the acceleration and deceleration of electrons emitted from 2<sup>nd</sup> inner iris can be clearly seen.

Supported by this result, in order to study the excitation condition of  $4/6 \pi$  mode triggered from the  $3/6 \pi$  mode, we employed the extensively used code ASTRA [9], with 3D field map imported from HFSS [10], to track the electrons in field of one mode and dual modes. The electric field maps of  $3/6 \pi$  and  $4/6 \pi$  mode are shown in Figure 5.

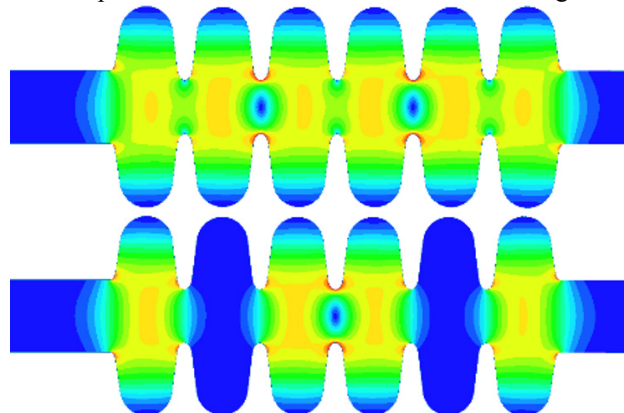


Figure 5: Electric field distribution in the ESS MB cavity (Upper:  $3/6 \pi$ ; Lower:  $4/6 \pi$ ).

### Electron Energy Gain

In theory, there are two possible electron energy-gain mechanisms: one due to the changing of the bunch trajectory by the excited passband-mode field, and the other due to modulation of the current by the excited mode field [6]. Since in our case the field of  $4/6 \pi$  mode is very low comparing to the  $3/6 \pi$  mode, the energy gain from current modulation will be negligible, and the main energy gain comes from the first mechanism.

In the simulation, we firstly calculate the electron impact energy in the fields of only  $3/6 \pi$  mode, and afterwards we calculate the same in the fields of dual-modes:  $3/6 \pi + 4/6 \pi$ . Subtracting the later to the former, we calculate the gain energy. A negative energy gain means a transfer of energy to the  $4/6 \pi$  mode.

The simulation starts from the four irises region. Each iris is scanned longitudinally in 30 points with a 2 mm step, marked as 0 to 29, symmetric to the iris centre, namely the closest points to iris centre are 14 to the left and 15 to the right. The maximum on-axis field is  $E_{1m} = 20$  MV/m for  $3/6 \pi$  mode and  $E_{2m} = 1$  MV/m for  $4/6 \pi$  mode. Usually, the input power is gradually increased during cavity vertical test. The FE is most likely to occur at the phase of maximum  $E_s$ . Due to this, we approximate all the electrons emitted at the  $0^\circ$  phase of driving mode, corresponding to the maximum field. The  $360^\circ$  phase of the passband mode is scanned each  $10^\circ$ .

Since FE strongly non-linearly depends on peak electric fields, it generally occurs in the highest  $E_s$  region:

$$J \approx \beta^{2.5} E_{peak}^{2.5} / \phi \exp(-6.53 \times 10^9 \frac{\phi^{1.5}}{\beta E_{peak}})$$

where  $J$  is the current density,  $\beta$  is the enhancement factor,  $\phi$  is the Fermi energy of the material and  $E_{peak}$  is the peak field on the surface.

For this reason, we assume that the electrons emit only from the sites with  $E_s$  higher than the 80% of the maximum  $E_s$  in the cavity (corresponding to more than 95 % of the total contribution to FE). In our case, this is equivalent to consider the centre of iris 0 and 2 in  $3/6 \pi$  mode.

The energy gained by the electrons emitted from the sites on iris-0 is shown in Figure 6, where the sites between the two red dashed lines show normalized  $E_s > 0.8$ . With this filtering criterion, we found that the most possible emission sites that transfer energy to the passband mode will be site 16 and 17 on iris-0 with an energy gain of about 20 keV.

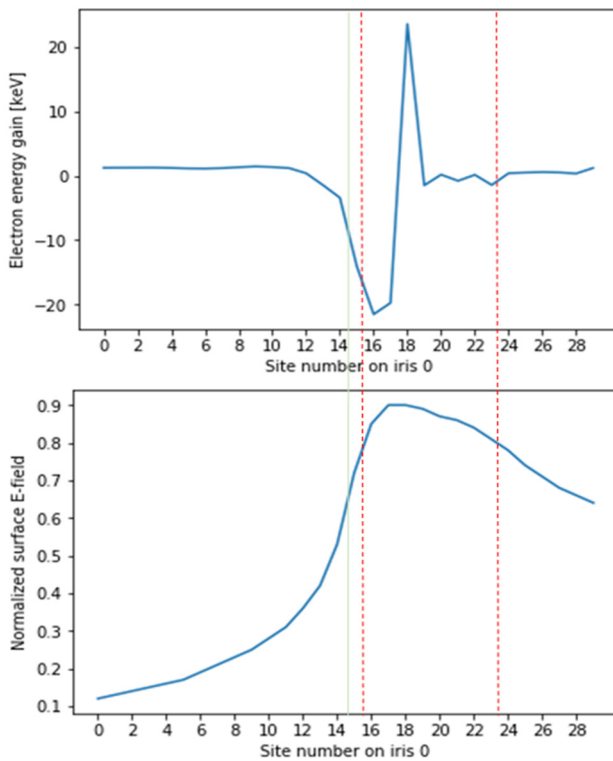


Figure 6: (Upper) Energy gain of electrons emitted from the sites on iris 0 (negative value denotes passing energy to excited mode); (Lower) normalized surface electric field of the sites on iris 0. Only sites between 16 and 23 have normalized  $E_s$  larger than 0.8. Green line denotes the iris centre.

The trajectories corresponding to the electrons emitted from site 16 and 17 on iris-0 are shown in Figure 7, where the multiple colourful trajectories correspond to different phases of the  $4/6 \pi$  mode at emission. As we can see, the energy gain takes place locally in the first cell.

Similarly, Fig. 8 shows the energy gain of electrons emitted from the sites on iris-2, and their corresponding  $E_s$ .

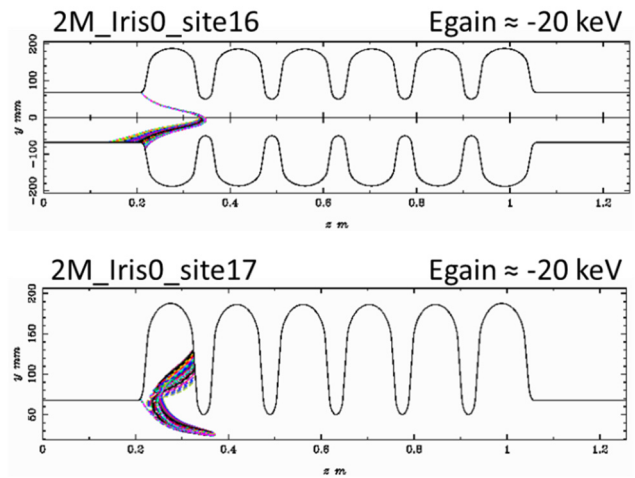


Figure 7: Trajectories of the electrons emitted from the sites with higher  $E_s$  on iris-0 (Upper: site 16; Lower: site 17).

This iris has the maximum  $E_s$  in the whole cavity. The normalized  $E_s$  of the all the 30 sites is larger than 0.8. Several sites show negative energy gain: the maximum energy gain is -200 keV at site 18 and the second one is -180 keV at site 23. The corresponding electron trajectories in the cavity are shown in Figure 9 and, the energy gain is mainly from the 3<sup>rd</sup> cell.

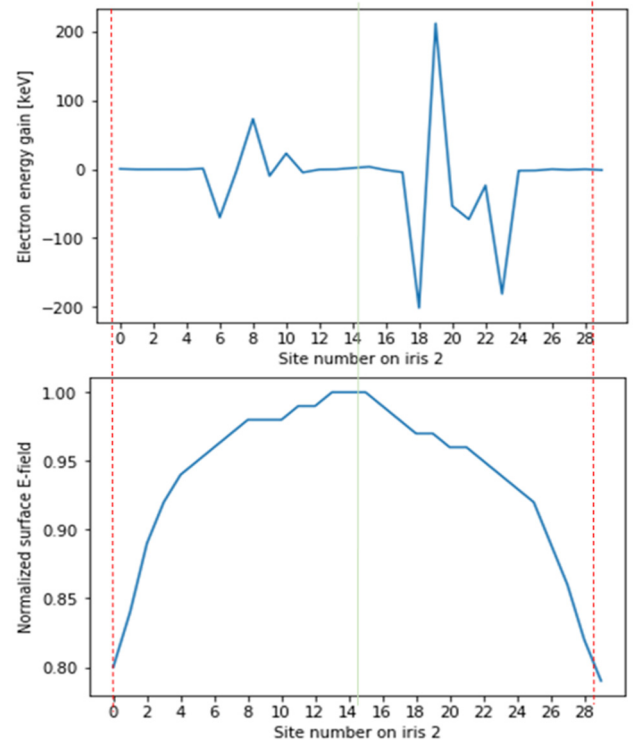


Figure 8: (Upper) Energy gain of electrons emitted from the sites on iris-2 (negative value denotes passing energy to secondary mode); (Lower) normalized surface electric field of the sites on iris-2. Green line denotes the iris centre; sites between two red dashed lines show normalized  $E_s > 0.8$ .



Content from this work may be used under the terms of the CC BY 3.0 licence (© 2017). Any distribution of this work must maintain attribution to the author(s), title of the work, publisher, and DOI.

Even if not on top of the dangerous iris list, we have analysed also the iris-1 and iris-3, as shown in Figure 10 and Figure 11 in appendix. Although the maximum energy gain in some sites are as large as -600 keV, we do not expect these sites as contributing to the passband mode excitation because their  $E_s$  are relatively too low to produce FE unless their field enhance factors are very high. Since we do not see any specific feature at these irises surface in the optical inspection, we assume that they have a same field enhance factor as other irises and hence are not source of FE.

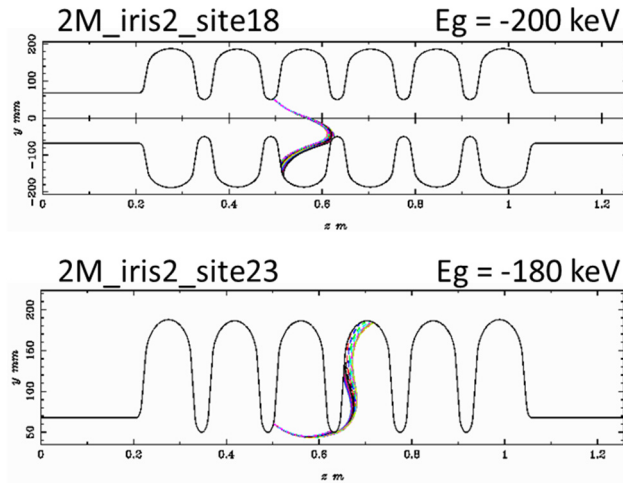


Figure 9: Trajectories of the electrons that emitted from the sites on iris-2 (Upper: site 18; Lower: site 23).

### Threshold Current

If the power gain is larger than the mode's dissipation on the cavity wall, the field will grow exponentially until it is limited by other mechanisms. This means the current of field emission should be large enough to excite the passband mode. The threshold current is [6]:

$$I_{th} = \omega U_i / Q V_i$$

where  $\omega$  and  $U_i$  are the angular frequency and the stored energy, respectively, of the excited mode, namely  $4/6 \pi$  mode in our case;  $Q$  is its quality factor of order  $10^{10}$  due to low external coupling in vertical test, and  $V_i$  is the equivalent voltage of energy gain.

Using frequency  $f = 701.80$  MHz in designed cavity, maximum  $V_i = 200$  kV from iris-2, store energy 78 mJ at  $E_{2m} = 1$  MV/m from Superfish, and assuming  $Q = 10^{10}$ , we can estimate the threshold current  $I_{th} = 0.2 \mu\text{A}$ . And  $I_{th} = 1.7 \mu\text{A}$  if the  $V_i = 20$  kV from iris-0, as shown in Table 1.

Table 1: Threshold Current of  $4\pi/6$ -mode Excitation

Parameters	Iris-2	Iris-0
$E_{2m}$ (MV/m)	1	1
$f$ (MHz)	701.8	701.8
$U_i$ (mJ)	78	78
$Q$	$10^{10}$	$10^{10}$
$V_i$ (kV)	200	20
$I_{th}$ ( $\mu\text{A}$ )	0.2	1.7

Considering both the threshold current and surface  $E_s$ , we find the site 18 on iris-2 is the most likely site among all the possible sites above, because it has the lowest threshold current and maximum surface  $E_s$ .

## CONCLUSION

Passband-mode triggered by field emission was observed in the 1<sup>st</sup> cold test of large grain cavity --  $4/6 \pi$  mode was excited spontaneously during the power rise of  $3/6 \pi$  mode. Simulation has been done to understand the scenario of this phenomenon. Some possible emission sites and corresponding electron trajectories are proposed, among which the most probable one is the site 18 on iris-2. The threshold current can be in the order of  $1 \mu\text{A}$ . Further studies on the reason of the excitation of mode  $4/6 \pi$  and on the possibility to see passband mode excitation in the fundamental  $\pi$  mode are undergoing.

## ACKNOWLEDGEMENT

The authors would like to thank Alberto Bacci for the discussion on the 3D-field-map transformation from HFSS to ASTRA and his support with his own code.

## APPENDIX

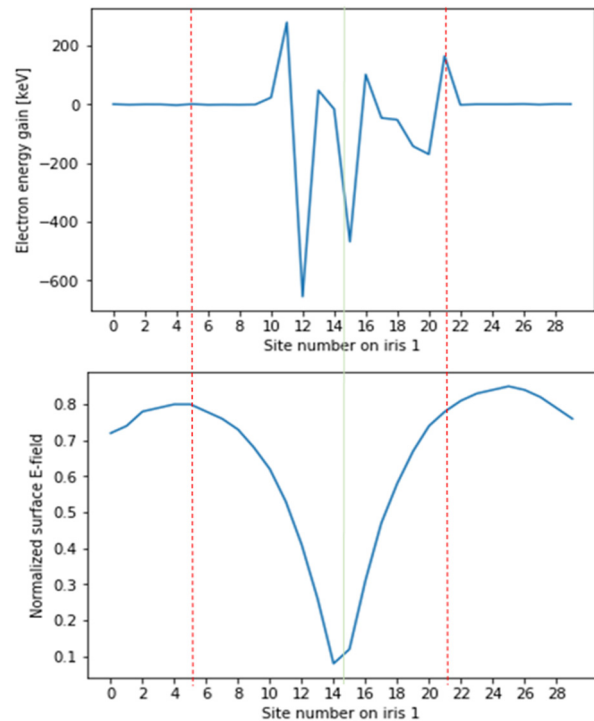


Figure 10: (Upper) Energy gain of electrons emitted from the sites on iris-1; (Lower) normalized surface electric field of the sites on iris-1.

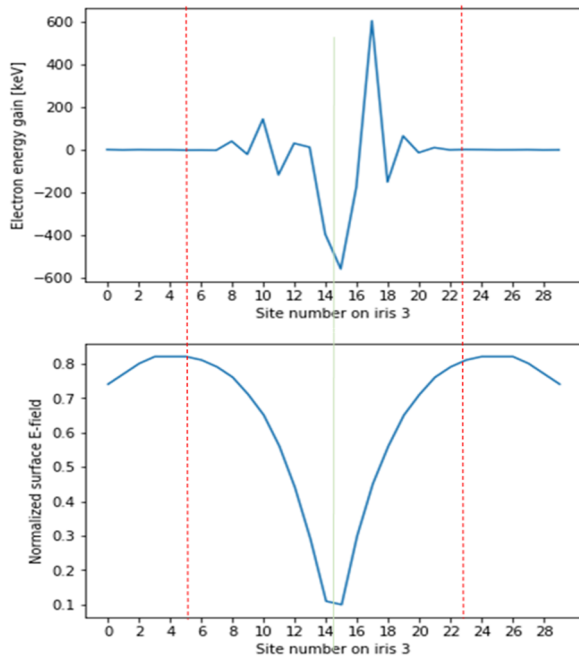


Figure 11: (Upper) Energy gain of electrons emitted from the sites on iris-3; (Lower) normalized surface electric field of the sites on iris-3.

## REFERENCES

- [1] A. Bosotti, *et al.*, "Vertical tests of ESS medium beta prototype cavities at LASA", in *Proc. IPAC'17*, Copenhagen, Denmark, 2017.
- [2] D. Sertore, *et al.*, "Experience on design, fabrication and testing of a large grain ESS medium beta prototype cavity", in *Proc. IPAC'17*, Copenhagen, Denmark, 2017.
- [3] J.F. Chen, *et al.*, "Multipacting Study in INFN-LASA ESS Medium-Beta Cavity", in *Proc. IPAC'17*, Copenhagen, Denmark, 2017.
- [4] G. Kreps, *et al.*, "Excitation of parasitic modes in cw cold tests of 1.3 GHz TESLA-type cavities", in *proc. SRF'09*, Berlin, Germany, 2009, TUPPO036.
- [5] P. Michelato, *et al.*, "ESS medium and high beta cavity prototypes ", in *Proc. IPAC'16*, Busan, Korea, May 8-13, 2016, p. 2138-2140.
- [6] V. Volkov, *et al.*, "Monopole passband excitation by field emitters in 9-cell TESLA-type cavities", *Phys. Rev. ST Accel. Beams*, vol. 13, p. 084201, Aug. 2010.
- [7] O. Fuks, "Excitation of passband modes in superconducting RF cavities", Technical note, Aug. 2012.
- [8] CST Particle Tracking Solver, CST GmbH, 2016
- [9] K. Floettmann, ASTRA, <http://www.desy.de/~mpyflo/Astra>
- [10] HFSS, <http://www.ansys.com/products/electronics/ansys-hfss>.